Gas-Phase Basicities of Acid Anhydrides

G. Bouchoux*

Département de Chimie, Laboratoire des Mécanismes Réactionnels, URA CNRS 1307, Ecole Polytechnique, 91128 Palaiseau Cedex, France

J.-F. Gal and P. C. Maria

GRECFO Chimie Physique Organique, Groupe FT-ICR, Université de Nice-Sophia Antipolis, 06108 Nice Cedex 2, France

J. E. Szulejko and T. B. McMahon

Department of Chemistry, University of Waterloo, Waterloo, Ontario N2L 3G1, Canada

J. Tortajada and A. Luna

Laboratoire de Chimie Structurale Organique, UMR CNRS 172, Université Pierre et Marie Curie (Paris VI), 4 Place Jussieu, Boite 45, 75252 Paris Cedex 05, France

M. Yàñez and O. Mó

Departamento de Quimica, Universidad Autonoma de Madrid, Cantoblanco, 28049 Madrid, Spain

Received: July 6, 1998; In Final Form: September 9, 1998

The gas-phase proton affinities (PA's) of acetic anhydride, **1**, and several representative cyclic anhydrides (succinic, **2**; methylsuccinic, **3**; glutaric, **4**; and 3-methylglutaric, **5**) were measured through the use of Fourier transform-ion cyclotron resonance and high-pressure chemical ionization techniques: PA(**1**) = 844 ± 1 kJ/mol, PA(**2**) = 797 ± 1 kJ/mol, PA(**3**) = 807 ± 1 kJ/mol, PA(**4**) = 816 ± 3 kJ/mol, PA(**5**) = 820 ± 3 kJ/mol. The results were analyzed in the light of molecular orbital ab initio (MP2/6-31G*, G2) and density functional theory (B3LYP/6-31G*) calculations. The enol forms of acetic ahydride and its protonated counterparts were predicted to be significantly less stable than the corresponding diketo conformers. The large proton affinity of acetic anhydride takes its origin from the formation of an intramolecular hydrogen bond in the protonated form. This is supported by the computational results and by the measurement of a sizable entropy loss upon protonation. In contrast, the protonation of cyclic anhydrides is accompanied by an acyl bond fission, thus leading to an entropy gain upon protonation. The protonated structures of cyclic anhydrides are stabilized by an electrostatic attraction between the two opposite parts of the ion. This effect is more pronounced for glutaric derivatives, and this explains the enhancement of the proton affinity observed when the size of the ring increases. It is also related to the increase in entropy of protonation and to the observed methyl substitution effect.

Introduction

One important characteristic of gas-phase ion chemistry is that the absence of solute/solvent interactions permits the deduction of intrinsic reactivities. It has been possible, in this way, not only to establish accurate gas-phase basicity and acidity scales[1−4] but also to investigate structural effects on the intrinsic reactivities of different families of compounds.[5] In the past few years we have been interested in the study of the intrinsic basicities of cyclic carbonyl bases: ketone,[6] lactams,[7] and lactones, saturated[8,9] or unsaturated.[10] We have found that the basicities of these systems increase with the size of the ring and are clearly different from those exhibited by the corresponding aliphatic homologues.These changes in the intrinsic basicities of cyclic carbonyl bases have several origins. On one hand, the size of the ring dictates the hybridization pattern of the carbonyl carbon. The smaller the angle (i.e., the smaller is the size of the ring), the greater is the electronegativity of the carbonyl carbon and consequently the lower is the electron donor ability of the carbonyl group. On the other hand, as the size of the ring increases, interfunctional interactions may be modified. For example, in the case of the lactones, the distance between the attaching proton and the negatively charged ether-like oxygen decreases when the size of the ring increases. The obvious consequence is that the stabilizing electrostatic interaction between these two atoms parallels the size of the ring.

The aim of this work is to go one step further by investigating the intrinsic basicities of another important series of carbonyl compounds: the acid anhydrides. It is well-known that this class of molecules is used in organic synthesis to prepare esters or amides by acylation of alcohols or amines under acidic conditions, and it is thus of interest to examine the structural effects on the intrinsic basicity of these compounds. In the present investigation, we hope to answer several questions: Do the gas-phase basicities of these compounds change significantly

10.1021/jp982877e CCC: $15.00
Published on Web 10/27/1998

SCHEME 1

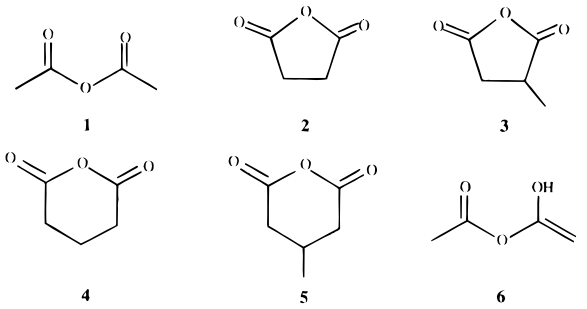

with the size of the ring? Are substituent effects similar to those found for other cyclic carbonyl compounds? Do any significant cyclization effects exist when the basicities of cyclic anhydrides are compared with those of aliphatic anydrides? For this purpose we have carried out a combined experimental and theoretical study on a series that includes the prototypes of aliphatic and cyclic anhydrides (Scheme 1). The set of compounds under consideration includes acetic anhydride, **1**, succinic anhydride, **2**, glutaric anhydride, **4**, and the methyl derivatives **3** and **5**. We have also considered theoretically the stability and the basicity of the enol tautomer of acetic anhydride, **6**.

The experimental gas-phase basicities of these systems were studied through the use of high-pressure mass spectrometry (HPMS) and Fourier transform-ion cyclotron resonance (FT-ICR) spectrometry. The results have been analyzed in the light of high-level ab initio and density functional theory (DFT) calculations.

Experimental and Computational Section

Equilibrium proton exchange measurements were conducted on two pulsed ionization high-pressure mass spectrometers (HPMS) constructed at the University of Waterloo, either configured around a modified VG 70-70 whose geometry was reversed to provide a B-E instrument or around a single magnetic sector VG 8-80. The apparatus and its capabilities have been described in detail previously.[11] The thermochemical data pertaining to **1** were measured on the VG 8-80 based HPMS, and that for **2**, **3**, **4**, and **5** were obtained on the VG 70-70 based HPMS.

Owing to the relatively low vapor pressure of the solid cyclic anhydrides (**2**, **3**, **4**, and **5**), the sample reservoir, leak valve, and the inlet line to the ion source were kept at ~90 °C. The cyclic anhydrides were dissolved in a large excess of benzene at known concentrations prior to injection into a 5 L metal reservoir. The resulting partial pressures of **2**, **3**, **4**, and **5** in the reservoir ranged from 0.05 to 0.15 Torr. The partial pressures of the reference bases used were in the range of 0.05−10 Torr, and methane (both the bath gas and the chemical ionization reagent gas) was added to ~1000 Torr total pressure. The contents of the reservoir were allowed to mix for ~30 min before the leak valve was opened. The mixture was flowed through the ion source at 5−10 Torr for at least 30 min before equilibrium measurements were attempted. This allowed for equilibration of **2**, **3**, **4**, and **5** on the surfaces of the low-pressure side of the leak valve, the inlet line, and the ion source walls. In this way the mole fraction of **2**, **3**, **4** and **5** both in the ion source and in the reservoir should be almost identical. No special procedures were used for the more volatile liquid anhydride, **1**.

FT-ICR experiments were carried out as described in detail elsewhere.[12] Briefly, proton-transfer equilibrium constants were measured at 338 K against pertinent reference bases. Sensitivities (S_r, relative to N_2) of the ionization gauge were estimated according to the method of Bartmess and Georgiadis:[13] $S_r = 0.36\alpha(\text{ahc}) + 0.30$, where α(ahc) is the average molecular polarizability based on atomic hybrid components calculated using the additivity scheme of Miller and Savchik.[14]

All chemicals used in the FT-ICR and HPMS measurements were of the highest purity commercially available, and they were utilized without further purification.

Standard ab initio and DFT calculations have been carried out using the Gaussian-94 series of programs.[15] Initially, the geometries of the different neutral and protonated species investigated were optimized at the HF/6-31G* level. These geometries were then refined at the MP2/6-31G* level to take explicitly into account electron correlation effects. The geometries of neutral and protonated species were also optimized using the B3LYP method and a 6-31G(d) expansion. The corresponding harmonic vibrational frequencies were calculated at the same level of theory as that used for the geometry optimizations. This allowed us to verify that the stationary points found were local minima on the potential energy surface and to calculate both the zero point energy (ZPE) and the entropy of the species considered. ZPE's calculated at the HF/6-31G* level were scaled by the empirical factor 0.893, while for those obtained at the B3LYP level, the 0.98 empirical factor proposed by Bauschlicher[16] was used.

It seems well established that calculated proton affinities in agreement with experimental values can only be attained at high ab initio levels. In this respect, the G2 theory has been shown to have a very good performance. Unfortunately, this level of calculation is too expensive for large systems such as those investigated here. Hence, for the unsubstituted cyclic anhydrides, namely, **2** and **4** and their protonated species, we have used the more economic G2(MP2, SVP) formalism, where the QCISD(T) component of the final energy is evaluated using a split-valence (SVP) 6-31G(d) basis set and the energy enhancements associated with high angular momentum basis and diffuse basis are obtained at the MP2 level. For the larger systems included in this study, this approach is still too expensive; hence, for these and the remaining systems under study, the final energies were also obtained at the B3LYP/6-311+G(3df,2p) level on the B3LYP/6-31G(d) optimized geometries. This theoretical scheme was found to provide protonation energies in good agreement with experimental values and with estimates obtained using high-level ab initio techniques in the framework of the G2 theory, for bases containing first-row and second row atoms.[17−19]

To investigate the bonding characteristics of the different species, we used the atoms in molecules (AIM) theory of Bader.[20] Using this approach, we have located the bond critical points (bcps), i.e., points where the electron density function, $\rho(r)$, is minimum along the bond path and maximum in the other two directions. The Laplacian of the density, $\nabla^2\rho(r)$, as has been shown in the literature, identifies regions of the space wherein the electronic charge is locally depleted ($\nabla^2\rho > 0$) or built up ($\nabla^2\rho < 0$). The former situation is typically associated with interactions between closed-shell systems (ionic bonds, hydrogen bonds, and van der Waals molecules), while the latter characterizes covalent bonds, where the electron density concentrates in the internuclear region. There are however significant exceptions to this general rule, mainly when high electronegativity atoms are involved in the bonding. Hence, we have also evaluated the energy density, $H(r)$, which does not present these exceptions. In general, negative values of $H(r)$

TABLE 1: Total Energies and Zero Point Vibrational Energies (ZPE) (in hartrees) for the Acid Anhydrides under Investigation

species[a]	MP2/6-31G*	B3LYP/6-31G*[b]	B3LYP/6-311+G(3df,2p)[b]	G2(MP2,SVP)	ZPE	PA(B3LYP)[c]	PA(G2)[c,d]
1a	−380.646 34	−381.727 88 (0)	−381.874 31 (0)		0.098 84	841	
1b	−380.645 47	−381.727 88 (1)	−381.874 15 (1)		0.099 15		
1c		−381.715 30 (32)			0.098 48		
TS1		−381.726 29 (4)	−381.873 39 (2)		0.098 67		
1aHa	−380.967 27	−382.059 20 (0)	−382.203 86 (0)		0.110 77		
1aHb	−380.961 60	−382.050 54 (21)	−382.197 46 (15)		0.109 92		
1bHa	−380.963 47	−382.053 83 (14)	−382.199 11 (12)		0.110 66		
1bHb	−380.957 26	−382.048 70 (27)	−382.195 08 (23)		0.110 72		
1bHc		−382.035 17 (55)	−382.187 14 (35)		0.107 56		
TS2		−382.041 73 (43)	−382.188 43 (37)		0.109 49		
2	−379.476 70	−380.523 07	−380.666 18	−379.865 15	0.085 97	799	792
2Ha	−379.785 13	−389.837 23	−380.979 04	−380.163 87	0.098 61		
2Hb	−379.755 80				0.095 59		
3	−418.651 48	−419.838 89	−419.994 49		0.116 24	809	
3Ha	−418.962 39	−420.156 00 (0)	−420.310 65 (2)		0.128 83		
3Hb	−418.963 21	−420.156 40 (0)	−420.311 20 (0)		0.128 72		
4	−418.644 54	−419.833 13	−419.988 63	−419.069 36	0.117 20	831	822
4Ha	−418.965 25	−420.159 50	−420.313 68	−419.379 97	0.129 77		
4Hb	−418.943 14				0.126 89		
5	−457.819 10	−459.148 80	−459.317 26		0.147 05	836	
5Ha	−458.141 48	−459.477 12	−459.644 30		0.159 63		
6		−381.692 77	−381.846 24		0.099 40		
6Ha		−382.017 07 (0)	−382.168 29 (0)		0.110 97		
6Hb		−382.007 73 (24)	−382.161 99 (16)		0.110 78		

[a] **1**, acetic anhydride; **2**, succinic anhydride; **3**, methylsuccinic anhydride; **4**, glutaric anhydride; **5**, 3-methylglutaric anhydride; **6**, enol form of acetic anhydride. [b] Values in parentheses correspond to relative energies including unscaled ZPE, in kJ/mol. [c] The calculated proton affinities (PA in kJ/mol) include thermal corections at 298 K. [d] G2 calculations were carried out at the G2(MP2,SVP) level of theory.

are associated with a stabilizing charge concentration within the bonding region. The AIM analysis was performed using the AIMPAC series of programs.[21]

The optimized geometries of the different systems included in this study are schematized in Figure 1. The corresponding total energies, as well as the calculated proton affinities, are summarized in Table 1.

Results and Discussion

Experimental Proton Affinities of 1−5. Experimental determination of the proton affinities of acid anhydrides **1**−**5** was done by the procedure of proton-transfer equilibrium measurement.[22] Proton-transfer reactions between the species under study, M, and a number of reference bases B (eq I) were performed on both the HPMS and the FTICR apparatus.

$$MH^+ + B \rightleftarrows M + BH^+ \qquad \text{(I)}$$

The equilibrium constant, K, of reaction I at a given temperature T is determined from the ratio of ion intensities, MH^+/BH^+, at equilibrium, and the partial pressure ratio of M and B. The corresponding standard free energy change, $\Delta G_T°$, is directly obtained from the equilibrium constant (eq II):

$$\Delta G_T° = -RT \ln K \qquad \text{(II)}$$

In FT-ICR experiments the equilibrium constants have been determined at a single temperature (T = 338 K). In such circumstances, the proton affinity of M, PA(M), may be deduced from the relationship (eq III)

$$\mathrm{PA(M)} = \mathrm{PA(B)} + \Delta G_T° + T[\Delta S°_{1/2}(\mathrm{B}) - \Delta S°_{1/2}(\mathrm{M})] \qquad \text{(III)}$$

where $\Delta S°_{1/2}$ is the difference in standard entropy between the protonated and the neutral species ($\Delta S°_{1/2}$ (X) = $\Delta S°(XH^+) - \Delta S°(X)$).

In HPMS experiments, both the entropy and enthalpy changes can be determined accurately from the variation of the equilibrium constant as a function of temperature. From a linear regression of a plot of ln(K) versus 1/T (eq IV), the slope yields $\Delta H°$ and the intercept, $\Delta S°$, where $\Delta H°$ and $\Delta S°$ refer to reaction I.

$$\ln K = -\Delta G°/RT = -\Delta H°/RT + \Delta S°/R \qquad \text{(IV)}$$

If PA(B) and $\Delta S°_{1/2}$(B) are well-established standards, then the unknown values are readily obtained from eqs V and VI:

$$\mathrm{PA(M)} = \mathrm{PA(B)} + \Delta H° \qquad \text{(V)}$$

$$\Delta S°_{1/2}(\mathrm{M}) = \Delta S°_{1/2}(\mathrm{B}) - \Delta S° \qquad \text{(VI)}$$

The experimental data involving proton-transfer reaction I (M = **1**−**5**) obtained from both HPMS and FT-ICR experiments are reported in Table 2. The $\Delta G°$ were determined by FT-ICR at T = 338K; the HPMS data shown in Table 1 were extrapolated to this temperature. For the reference bases B, PA(B) and $\Delta S°_{1/2}$(B) were taken from the published data of Szulejko and McMahon.[4] The PA(M) values were calculated using either eq III or V depending upon the experimental method used. Excellent agreement between the PA(M) values derived from FTICR and HPMS has been obtained, particularly for **2** and **3**. In the case of **4** and **5** a systematic difference of 3−7 kJ·mol^{-1} is observed. However, for these two compounds, the uncertainty in GB reaches ±3 kJ·mol^{-1} owing to more severe volatility constraints.

A first general observation that emerges from examination of Table 2 is that acetic anhydride, **1**, behaves differently from the cyclic acid anhydrides **2**−**5**: **1** is the most basic compound

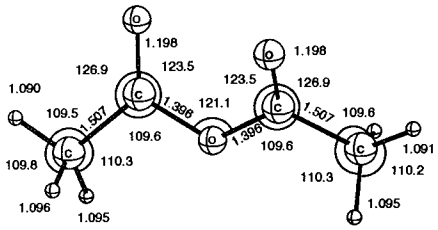

1a

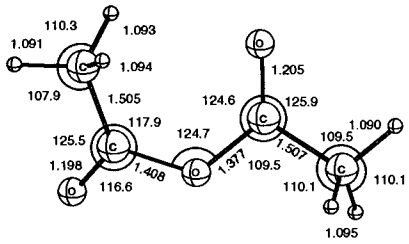

1b

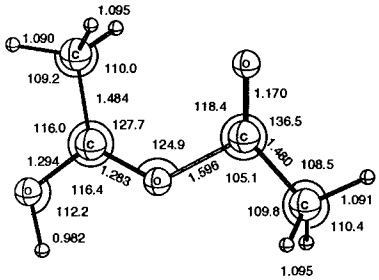

1bHa

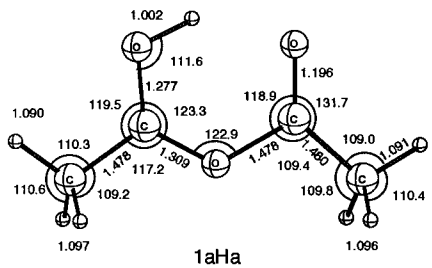

1aHa

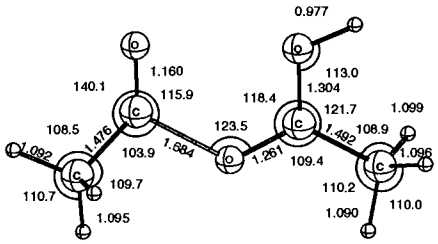

1aHb

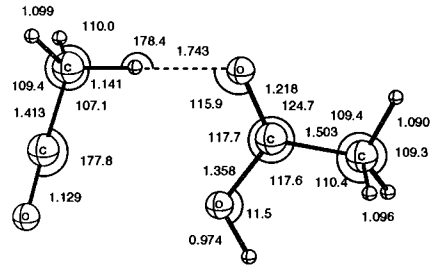

1bHc

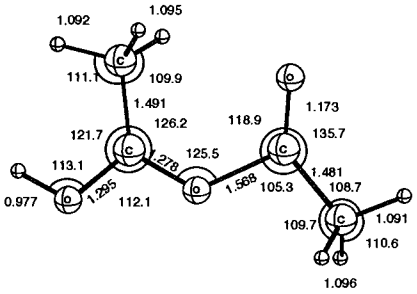

1bHb

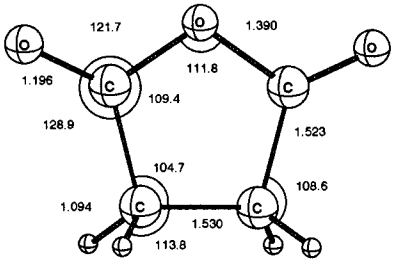

2

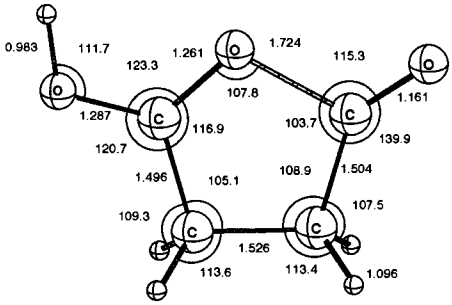

2Ha

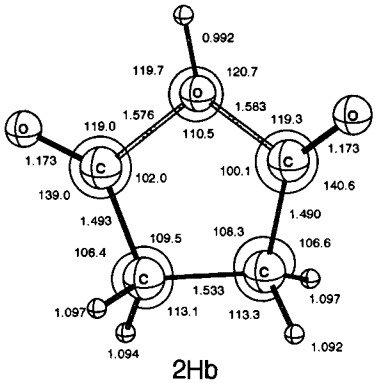

2Hb

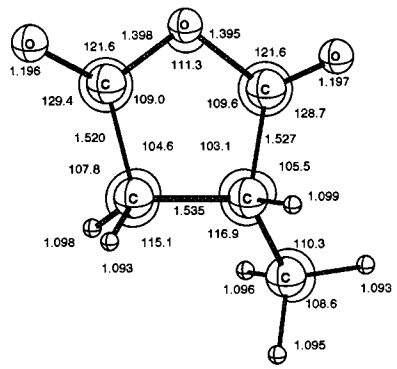

3

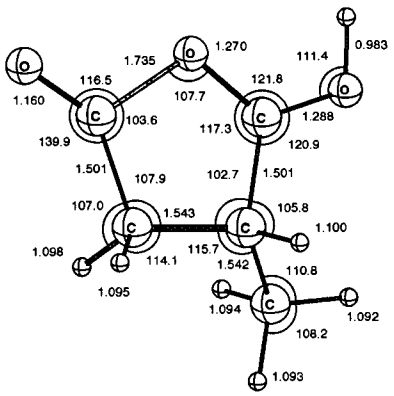

3Ha

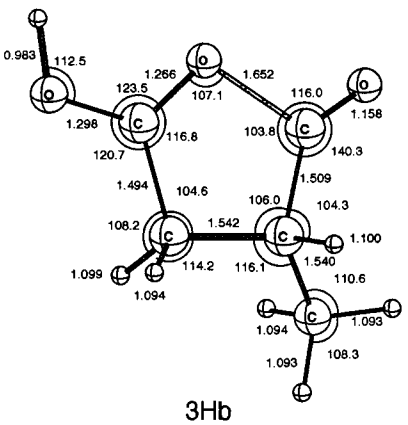

3Hb

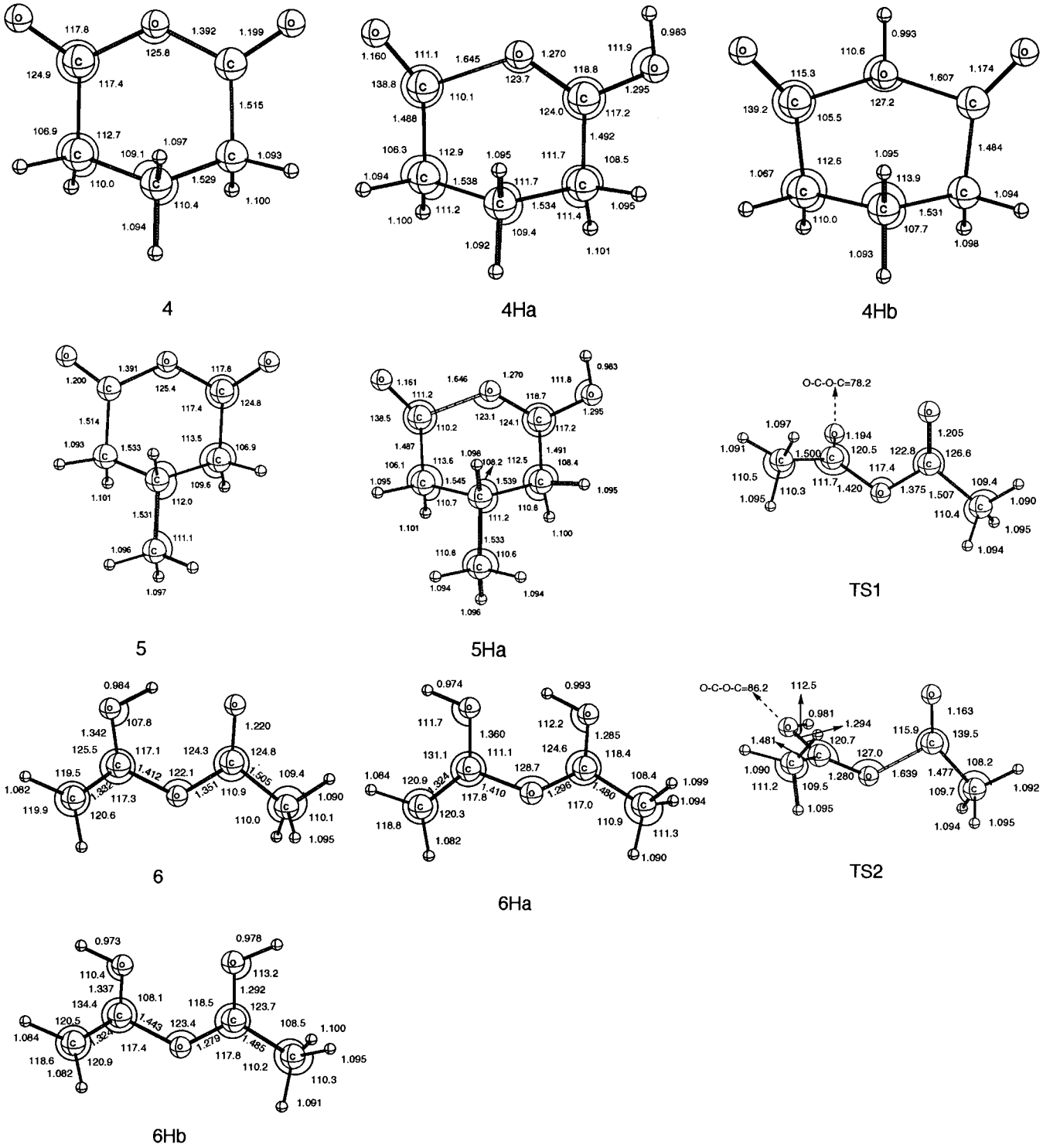

Figure 1. Geometrical parameters of the neutral and protonated forms of anhydrides **1**−**6** (B3LYP/6-31G* except for **2Hb** and **4Hb** for which MP2/6-31G* values are reported).

and the only one to possess a negative protonation entropy, $\Delta S°_{1/2}$. Second, it clearly appears that the proton affinities of the cyclic anhydrides increase as the size of the ring increases. This influence of the ring size is in line with the one described for other cyclic carbonyl bases. It is worth noting, however, that this increase in basicity is accompanied by an increase in the $\Delta S°_{1/2}$ term. Moreover, the latter becomes as high as ∼35 $J \cdot mol^{-1} \cdot K^{-1}$ for the glutaric derivatives **4** and **5**, thus pointing to a substantial structural change upon protonation. Finally, the role of the methyl substitution appears to be appreciable only for the succinic derivative, **3**. These essential trends will be discussed in the following sections in conjunction with the presentation of the computational results.

Protonation of Acetic Anhydride, 1. Regarding acetic anhydride, the first important result is that the conformer **1c** (Scheme 2), which presents an atomic arrangement similar to that exhibited by the cyclic anhydrides, does not correspond to a local minimum of the potential energy surface at the MP2/6-31G* level.

We were able to locate a stationary point for this conformation at the B3LYP/6-31G* level of theory, but it was found to have one imaginary frequency corresponding to the rotation of one

TABLE 2: Equilibrium Proton Transfer Thermochemical Data for the Reaction $[MH]^+ + B \rightarrow M + [BH]^+$, M = Anhydrides 1−5[a]

M	B	method	$\Delta H°$	$\Delta S°$	$\Delta G°_{338}$	$\Delta S°_{1/2}$(B)[b]	$\Delta S°_{1/2}$(M)[c]	PA(B)[b]	PA(M)[d]
1	acetone	HPMS	33.5	68.2	10.5	16.7	−49.4	811.7	844.3
	isopropylcyanide	HPMS	41.0	61.9	20.1	12.6	−47.3	804.6	844.7
2	toluene	HPMS	10.0	10.0	6.7	20.9	2.5	784.1	797.1
	benzene	HPMS	42.7	13.4	38.5	27.2	7.5	751.4	796.6
	ethylformate	FT-ICR			−3.3	16.7	5.0	797.1	797.5
	butanal	FT-ICR			3.8	(16.7)[e]	5.0	785.3	797.1
	pentanal	FT-ICR			−1.3	(16.7)[e]	5.0	793.7	796.2
3	toluene	HPMS	20.5	7.5	18.0	20.9	5.0	784.1	807.5
	ethylformate	HPMS	9.2	6.3	7.1	16.7	10.5	797.1	806.3
	ethylformate	FT-ICR			6.7	16.7	7.5	797.1	806.7
	isopropylcyanide	FT-ICR			1.3	12.6	7.5	804.6	807.5
	cyclopropylcyanide	FT-ICR			−3.3	(12.6)[e]	7.5	807.9	806.2
4	acetone	HPMS	1.7	−18.4	7.9	16.7	37.2	811.7	812.5
	m-xylene	HPMS	10.0	2.1	9.2	33.5	31.4	804.2	814.2
	acetone	FT-ICR			10.0	16.7	34.3	811.7	815.9
	methyl acetate	FT-ICR			5.9	18.8	34.3	816.7	817.1
	diethyl ether	FT-ICR			−3.3	14.6	34.3	828.9	818.8
5	methyl acetate	HPMS	−0.4	−16.3	5.4	18.8	33.0	816.7	817.1
	m-xylene	HPMS	14.6	−0.4	14.6	33.5	33.9	816.7	818.8
	ethyl acetate	HPMS	−12.6	−22.6	−5.0	14.6	39.3	829.7	816.3
	mesitylene	HPMS	−12.6	−5.0	−10.9	27.2	30.1	830.5	818.8
	3-pentanone	HPMS	−15.9	−20.5	−8.8	12.6	29.7	824.7	820.0
	diethyl ether	FT-ICR			1.7	14.6	33.0	828.9	824.2
	ethyl acetate	FT-ICR			−0.8	14.6	33.0	829.7	822.6
	3-pentanone	FT-ICR			−4.2	12.6	33.0	824.7	823.4

[a] **1**, acetic anhydride; **2**, succinic anhydride; **3**, methylsuccinic anhydride; **4**, glutaric anhydride; **5**, 3-methylglutaric anhydride. $\Delta H°$, $\Delta G°$, PA, and GB in kJ·mol^{-1}; $\Delta S°$ in J·mol^{-1}·K^{-1}. [b] Unless otherwise noted, $\Delta S°_{1/2}(B) = S°(BH^+) - S°(B)$ and PA(B) are taken from ref 4 and later additional unpublished data. A few minor revision/corrections have been made to the data originally published. [c] $\Delta S°_{1/2}(M) = \Delta S°_{1/2}(B) - \Delta S°$ for HPMS experiments; the mean values derived from HPMS measurements are used with the FT-ICR data. [d] $PA(M) = PA(B) + \Delta H°$ for HPMS data, and $PA(M) = PA(B) + \Delta G_T° + T[\Delta S°_{1/2}(B) - \Delta S°_{1/2}(M)]$ ($T = 338$ K) for FT-ICR data. [e] $\Delta S°_{1/2} = \Delta S°_{1/2}$ (ethyl formate) = 16.7 J·mol^{-1}·K^{-1} has been assigned to butanal (isoelectronic analog) and pentanal; $\Delta S°_{1/2} = \Delta S°_{1/2}$(isopropyl cyanide) = 12.6 J·mol^{-1}·K^{-1} has been assigned to cyclopropyl cyanide. For these compounds, PA(B) have been reestimated from the data tabulated in ref 1 and anchored to the new standard PA(isobutene) = 802.1 kJ·mol^{-1}, $\Delta S°_{1/2}$ (isobutene) = 23.0 J·mol^{-1}·K^{-1} (ref 4); the derived PA(B) values are indicated in parentheses.

SCHEME 2

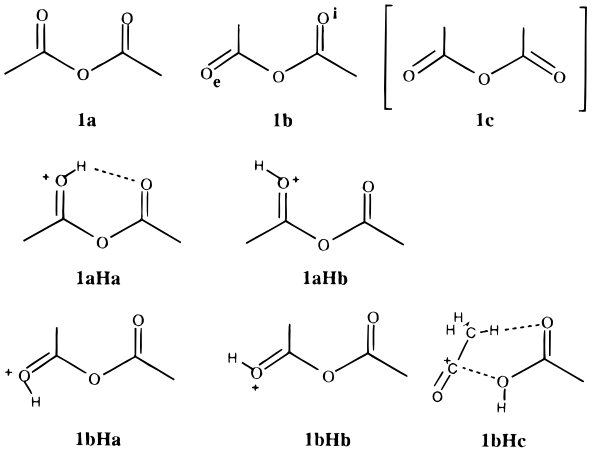

acyl moiety. All attempts to optimize a similar structure at the MP2/6-31G* level failed, since they collapsed to the local minimum **1b** (Scheme 2). In fact **1c** must be considered as the transition structure for the rotation around the O−CO$_i$ bond in **1b**. The calculated energy barrier, ca. 33 kJ/mol (B3LYP/6-31G*+ZPE), is significantly less than the 54 kJ/mol associated with the rotation around the O−CO bond in methyl acetate.[23] This is expected since the π-bond character of the O−CO bond is lower in **1b** than in methyl acetate.

The two stable conformers of the acetic anhydride, **1b** and **1a** (Scheme 2, Figure 1), are predicted to be of comparable energy (Table 1). It may be noted that the strong repulsions between the lone pairs of the neighboring oxygen atoms lead, in both cases, to nonplanar conformations where the two carbonyl groups do not lie in the same plane (Figure 1). Interestingly enough, the O−CO bond lengths are identical in **1a** (1.396 Å) and significantly different in **1b**. In the latter structure, the O−CO$_i$ bond (1.377 Å) exhibits a clear π-bond character while the O−CO$_e$ bond (1.408 Å) is close to a pure σ-bond. This explains why the rotation around the O−CO$_i$ bond needs more energy than the rotation around the O−CO$_e$ bond. Accordingly, a rotational barrier of only 2 kJ/mol is calculated (B3LYP/6-311+G(3df,2p)+ZPE, **TS1**, Table 1) for the conformational change that involves the rotation around the O−CO$_e$ bond while, as discussed above, a barrier of 33 kJ/mol is associated with the rotation around the O−CO$_i$ bond.

Protonation of acetic anhydride may occur either at carbonyl oxygen or at the central, ether-like, oxygen. Starting from the conformer **1a** where the two carbonyl groups play symmetrical roles, protonation on the carbonyl leads to **1aHa** (Scheme 2, Figure 1), which is the most stable protonated species owing to the formation of an intramolecular hydrogen bond. The AIM theory reveals that this intramolecular hydrogen bond is not very strong: in fact the value of the charge density within the corresponding bonding region (O6···H, Figure 2) is almost twice that found for the intermolecular hydrogen bonds in water trimer[24] and almost identical to that found for the intramolecular hydrogen bond in thiomalonaldehyde,[25] i.e., for neutral systems. A confirmation of the weakness of the intramolecular hydrogen bond in protonated acetic anhydride is offered by the fact that the rotamers **1aHb**, **1bHa,** and **1bHb** (Scheme 2) are predicted to be only 15−30 kJ/mol above **1aHa** (Table 1). By comparison, the enthalpy gain upon protonation of 1,3-propanediol or 1,3-methoxypropanol (leading also to a six-membered cyclic protonated structure) is in the range 60−80kJ/mol.[26−28] Another observation is that he structure **1aHb** is characterized by an exceptionally long length of the C−O bond opposite to the

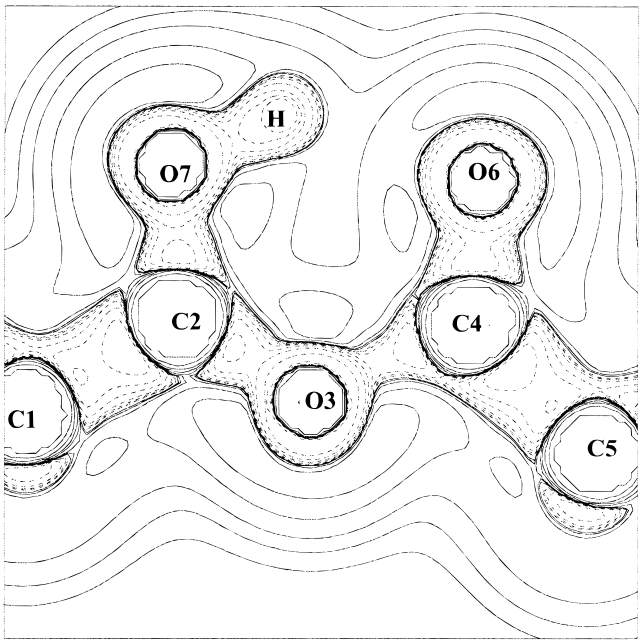

Bond	ρ	$\nabla^2\rho$	H(**r**)
C1-C2	0.273	-0.768	-0.286
C2-O3	0.328	-0.291	-0.543
O3-C4	0.213	-0.384	-0.244
C4-C5	0.269	-0.737	-0.274
C4-O6	0.417	0.360	-0.722
C2-O7	0.350	-0.155	-0.586
O7-H	0.298	-1.612	-0.459
O6....H	0.040	0.135	-0.001

Figure 2. Electron density (ρ), Laplacian ($\nabla^2\rho$), and energy density ($H(r)$) calculated for protonated acetic anhydride **1Ha**.

SCHEME 3

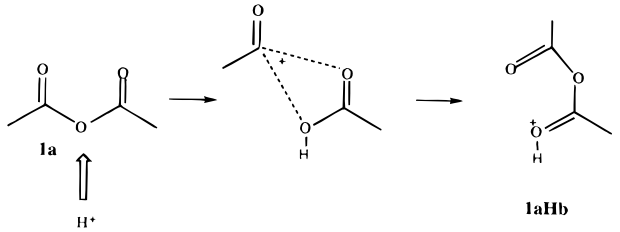

protonated group (1.684 Å, Figure 1). By contrast the other C−O bond is shortened to 1.261 Å. Thus, structure **1aHb** may be considered as a nascent complex between the acylium cation $[CH_3CO]^+$ and neutral acetic acid. A similar, though limited, effect appears also for structure **1aHa** as illustrated by the difference in C−O bond lengths (Figure 1) or by the charge density in the corresponding regions (see ρ(C2−O3) = 0.328 and ρ(O3−C4) = 0.213, Figure 2).

The conformation expected to arise from the protonation of **1a** at the ether-like oxygen is not stable. Interestingly enough, all attempts at geometry optimization collapse to structure **1aHb** along a path that involves, in a first step, the cleavage of one of the C−O acyl bond, yielding an acylium ion $[CH_3CO]^+$ and a CH_3COOH molecule in electrostatic interaction (Scheme 3). The subsequent step consists of the shift of the acylium subunit onto the carbonyl oxygen atom of the acetic acid moiety leading to species **1aHb**.

The three oxygen atoms of the conformer **1b** may a priori play distinct roles during the protonation, and consequently, five possible protonated structures have been explored. It is found that protonation at the "external" carbonyl (**e**, Scheme 2) could give rise to structures **1bHa** and **1bHb** (Scheme 2, Figure 1). The greater stability of the former structure is due to the favorable interaction between the proton and the ether-like oxygen. A similar stabilizing effect has been demonstrated for esters and lactones.[9,10] It may be noted, here also, that both structures **1bHa** and **1bHb** are characterized by an elongation of the C−O bond remote to the protonated acyl group (1.568 and 1.596 Å, respectively, Figure 1). Protonation at the "internal" carbonyl of the neutral **1b** (**i**, Scheme 2) leads to the protonated forms **1aHa** or **1aHb** after rotation of the second acyl group.

Finally, it can also be observed that protonation at the ether-like oxygen atom of the conformer **1b**, similarly to what has been found for **1a**, leads to the dissociation of one of the acyl C−O bonds. However, in this case, the species **1bHc** (Scheme 2 and Figure 1), which is a pure ion/dipole complex formed by one molecule of acetic acid and the $[CH_3CO]^+$ cation, is formed because the orientation of the methyl group of the acylium moiety favors the formation of a hydrogen bond with the carbonyl oxygen atom of the acetic acid subunit.

An important energetic parameter, pertaining to the protonation of acetic anhydride, is the rotational barrier associated with the conformational change involving the two most stable protonated forms accessible from **1a** and **1b**, i.e., the reaction **1aHa** → **1bHa**. The calculation predicts a barrier height of 37 kJ/mol for this reaction at the B3LYP/6-311+G(3df,2p) level (**TS2**, Table 2).

The enol form of the acetic anhydride, **6**, is predicted to be significantly less stable than the keto forms **1a** and **1b** (ca. 75 kJ/mol, Table 1). Protonation of structure **6** can take place either at an oxygen atom or at the methylene group. The most stable protonated forms are those that retain an intramolecular hydrogen bond, i.e., structures **6Ha** and **1aHa**, respectively (Figure 1). It is interesting to note, however, that the alternative conformation **6Hb** (Figure 1), where the internal hydrogen bond is broken, is ca. 16 kJ/mol above **6Ha** indicating also here a moderate internal hydrogen bond energy. In any case, the large instability of structure **6** with respect to **1** leads to the complete exclusion of the participation of the enol form of acetic anhydride during its protonation at thermal equilibrium.

The experimentally determined proton affinity of acetic anhydride is equal to 844 kJ/mol. Molecular orbital calculations give comparable results; an energy difference of 841 kJ/mol (B3LYP/6-311+G(3df,2p)+ZPE) is calculated between **1a** (or **1b**) and **1aHa**. This agreement must be discussed in line with the populations of both the neutral and the protonated forms. At room temperature the mean internal energy of acetic anhydride is ca. 20 kJ/mol. This value is greater than the energy barrier separating **1a** and **1b** (2 kJ/mol, see above) and allows both structures to be in equilibrium during protonation. Concerning the protonated forms, the easiest conformational change, **1aHa** → **1bHa**, requires 37 kJ/mol and is thus not expected to occur at a fast rate. The most stable protonated form being **1aHa**, the participation of the conformer **1bHa** may be neglected.

In fact the situation is such that the neutral molecule **1** exhibits free internal rotations while the protonated structure **1aHa** is constrained by an internal hydrogen bond. This fact leads to two consequences: (i) the proton affinity value contains an extra term due to the internal hydrogen bond energy, and (ii) the difference in entropy between the protonated and the neutral forms should be negative. This is indeed the case. First, PA(**1**) (844 kJ/mol, Table 2) is clearly larger than the proton affinity

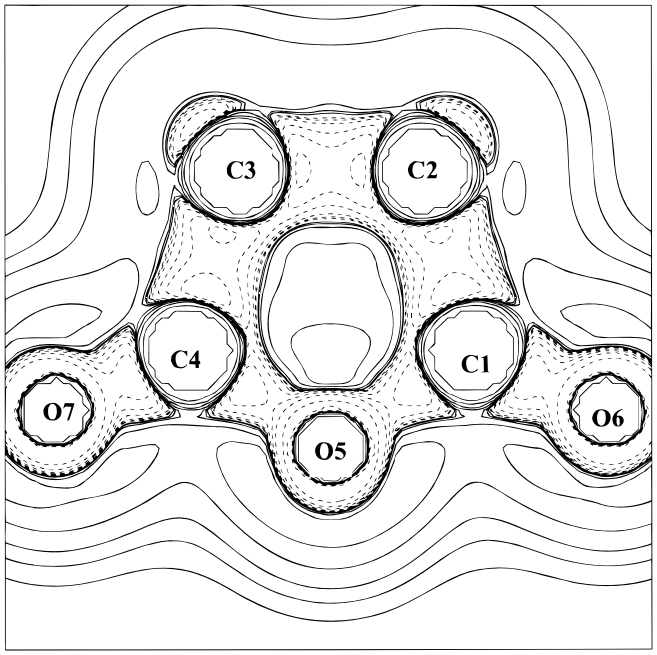

Bond	ρ	$\nabla^2\rho$	H(r)
C1-O5	0.273	-0.532	-0.414
C1-C2	0.258	-0.636	-0.228
C2-C3	0.248	-0.578	-0.208
C1-O6	0.416	0.272	-0.722

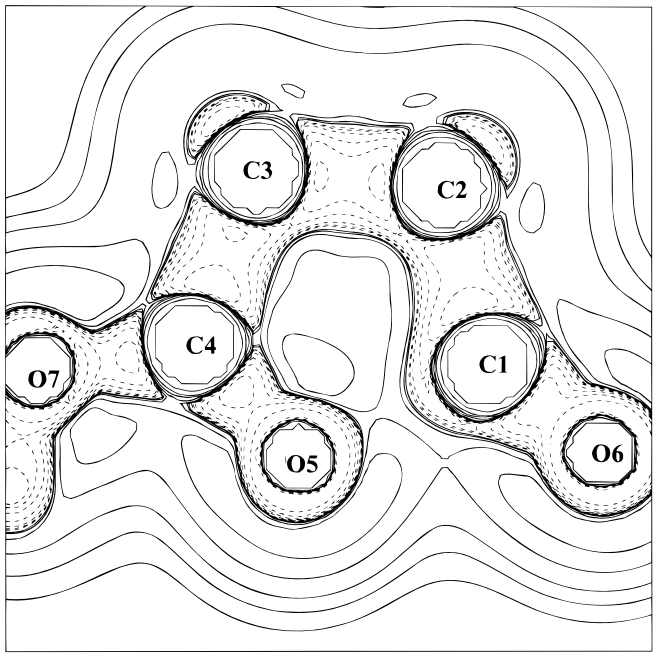

Bond	ρ	$\nabla^2\rho$	H(r)
C1-O5	0.130	0.081	-0.060
C1-O6	0.449	-0.877	-0.775
C1-C2	0.254	-0.636	-0.243
C2-C3	0.246	-0.572	-0.205
C3-C4	0.268	-0.699	-0.253
C4-O5	0.368	-0.102	-0.628
C4-O7	0.339	-0.239	-0.564
O7-H	0.314	-1.702	-0.480

Figure 3. Electron density (ρ), Laplacian ($\nabla^2\rho$), and energy density ($H(r)$) calculated for (a) neutral succinic anhydride **2** and (b) protonated succinic anhydride **2Ha**.

of an acid (e.g., PA(CH_3COOH) = 789 kJ/mol, ref 1) or even of an ester such as methyl acetate (PA(CH_3COOCH_3) = 816 kJ/mol, ref 4). Second, the $\Delta S°_{1/2}$ term for acetic anhydride is equal to -48 J·mol^{-1}·K^{-1} (Table 2). This value is comparable to the entropy change determined for the protonation of 1,3-propanediol (-50 J·mol^{-1}·K^{-1}, ref 26) or 1,3-methoxypropanol (-59 J·mol^{-1}·K^{-1}, ref 28), in perfect agreement with a cyclic arrangement involving six atoms during the formation of the internal hydrogen bond.

Protonation of Cyclic Anhydrides. Protonation of the cyclic anhydrides at one of the carbonyl oxygen atoms results in the fission of the farthest C−O bond. This bond cleavage is, however, not complete, so, in general, the protonated species exhibits a quite distorted cyclic structure. This bond fission process can be understood by looking at the electronic redistribution undergone by the base after protonation, and which is clearly illustrated by comparing the Laplacian maps of the neutral and the protonated species. This was done in Figure 3 for the particular case of succinic anhydride, **2**, taken as a suitable model system.

In the protonation process, a large transfer of charge density (of about half an electron) takes place from the base onto the attaching proton. The most obvious result is that the C═O double bond becomes essentially a single bond in the protonated form. This is reflected by a lower charge density at the corresponding bond critical point (see ρ(C4−O7) = 0.416 for **2** and 0.339 in the case of **2Ha**, Figure 3). This polarization is also reflected by an increase of the charge density at the C4−O5 bond in which the carbonyl carbon participates. The accumulation of charge density into this bonding region implies a concomitant depletion of charge density from the other bonds, particularly in the O5−C1 acyl bond, which is practically broken (see Figure 3).

SCHEME 4

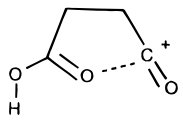

2Ha

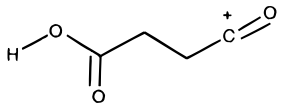

2Ha'

It is worth noting, however, that the protonated species retains a cyclic arrangement. Actually we have estimated for the particular case of species **2Ha** that the conformation depicted in Figure 2 is 52 kJ/mol more stable than the open-chain rotamer **2Ha′**. This is easily understood if one takes into account that, in its cyclic arrangement, the protonated form implies a favorable electrostatic interaction between the carboxylic acid group and the positive charge of the acylium moiety (Scheme 4).

The values of the charge density and the density of energy at the O5−C1 bond critical point confirm this analysis, in the sense that the former is much smaller than in a normal C−O covalent linkage, while the energy density is almost positive, which is typical of electrostatic interactions. Furthermore, the C1−O6 linkage has a substantial triple-bond character as expected for an acylium ion. This is reflected by values of the charge density and the energy density, which are significantly larger than those typically associated with C═O double bonds. To summarize, the significant loosening of the O5−C1 bond is compensated by the strenghtening of the C1−O6 bond. Thus it may be considered that the formation of a stable acylium

moiety is the driving force for the partial ring opening observed upon protonation on the carbonyl of cyclic anhydrides.

Figure 1 also shows that the protonation of the cyclic anhydrides at the ring oxygen atoms (**2Hb** and **4Hb**) retains the cyclic structure of the neutral, although both C−O bonds become significantly longer. Again this is a reflection of the charge density redistribution associated with the protonation process. As mentioned above there is a strong transfer of charge density from the oxygen atom to the attaching proton, and the former recovers part of this charge by depopulating the two C−O bonds in which it participates, which, accordingly, become weaker and longer. The corresponding protonated forms are substantially higher in energy than the carbonyl protonated isomers; the energy difference amounts to 77 kJ/mol for succinic anhydride, **2**, and 58 kJ/mol for glutaric anhydride, **4**. The highest value for the former includes the strain energy of the five-membered ring in **2Ha**. Finally, it is observed that protonation of methylsuccinic anhydride, **3**, on the carbonyl group yields two different isomers, namely **3Ha** and **3Hb**, of comparable energies (Table 1).

From both the experimental and the calculated proton affinities, it is apparent that the intrinsic basicities of cyclic anhydrides exhibit a similar dependence on the size of the ring as found for other cyclic carbonyl bases such as saturated and unsaturated lactones.[8−10] As shown in Table 2, glutaric anhydride, **4**, is 19 kJ/mol more basic than succinic anhydride, **2**. The calculated difference in proton affinities amounts to 30 kJ/mol (G2)/32 kJ/mol (B3LYP/6-31G*) (Table 1). This difference is of the same order of magnitude as that reported in the literature for the lactones (29 kJ/mol), or for α,β-unsaturated lactones (26 kJ/mol). However, the reason for this basicity enhancement with the size of the ring is here completely different. In the case of the cyclic anhydrides investigated here, the calculation demonstrates, and the experiment confirms, that the cyclic structure is radically modified upon protonation. The protonated form is a partially opened structure that gains its stability in an electrostatic interaction between an acyl ion and a carbonyl oxygen. This bonding interaction is, however, counterbalanced by the ring strain as illustrated by the fact that the elongated OC−O bond is equal to 1.72 Å in **2Ha** and only 1.61 Å in **4Ha** (see Figure 1). Consequently, the energy gain is higher in the case of **4Ha**, thus explaining the larger basicity observed for the glutaric anhydride **4**.

It can be also observed that the measured and calculated proton affinities show interesting methyl substituent effects. On going from **2** to **3** one notes a proton affinity increase of 9 kJ/mol (experiment, Table 2)/10 kJ/mol (B3LYP/6-31G* calculation, Table 1), which is a typical enhancement associated with the polarizability of a methyl group. However, both the experimental and the calculated values agree with a moderate proton affinity change on going from **4** to **5**: 4 kJ/mol (experiment, Table 2) and 5 kJ/mol (B3LYP/6-31G* calculation, Table 1). This can be explained if one takes into account that, as discussed before, the protonation at one of the carbonyl carbons leads to a bond fission that yields an acyl cation. In the protonated forms of species **3** (**3Hb**), the carbon of the methyl group is at a distance of 2.516 Å (B3LYP/6-31G*) from the positive charge, while in species **5Ha** this distance amounts to 3.874 Å (B3LYP/6-31G*). Since the stabilization energy associated with polarization interactions decreases as the fourth power of the distance, a much smaller stabilizing effect should be expected in the latter case where the substituent is quite far from the positively charged carbon.

Conclusions

A thorough experimental and theoretical study on the protonation of representative aliphatic and cyclic anhydrides has been carried out. The following important conclusions emerge.

(1) Both aliphatic and cyclic anhydrides behave as carbonyl bases in the gas-phase. Protonation on the central "ether-like" oxygen leads to structures of high energy or to dissociation.

(2) Acetic anhydride, **1**, is the most basic species of the series (PA = 844 kJ/mol). Its enol form, **6**, is predicted to be significantly less stable than the diketo forms. The corresponding protonated structures are also of low stability as compared with those obtained from the protonation of the diketo structures. The enhanced stability of the latter is directly related to the formation of strong intramolecular hydrogen bonds, which on one hand stabilizes the system and on the other hand leads to a significant decrease of the entropy of the system.

(3) Protonation of succinic, **2**, and glutaric, **4**, anhydrides, and their methyl derivatives, **3** and **5**, is accompanied by an acyl bond fission. This leads to a distorted protonated structure, which takes part of its stability from a favorable electrostatic interaction between the positive charge of the acyl moiety and the oxygen of the developing carbonyl group. This structure is characterized by a larger entropy than in its neutral, cyclic, counterpart. The six-membered ring leads to a more flexible structure, which affords (i) a greater stability owing to a more efficient internal electrostatic interaction and (ii) a marked increase in entropy upon protonation. The former point explains the increase of proton affinity with increasing ring size.

(4) The observed methyl substitution effect is also related to the aforementioned bond fission mechanism. The increase of the proton affinity due to the stabilizing effect of the methyl substituent on the protonated form depends strongly on its relative position within the molecule. This explains why this effect is only noticeable for the smallest ring system (methylsuccinic anhydride, **3**) where the methyl group is close to the positive charge.

Acknowledgment. M.Y. and O.M. acknowledge financial support from the Dirección General de Enseñanza Superior, Project No. PB96-0067.

References and Notes

(1) Lias, S. G.; Liebman, J. F.; Levin, R. D. *J. Phys. Chem. Ref. Data* **1984**, *13*, 695.

(2) Lias, S. G.; Bartmess, J. E.; Liebman, J. F.; Holmes, J. L.; Levin, R. D.; Mallard, W. G. *J. Phys. Chem. Ref. Data, Suppl. 1* **1988**, 17.

(3) Hunter, E. P.; Lias, S. G. http://webbook.nist.gov.

(4) Szulejko, J. E.; McMahon, T. B. *J. Am. Chem. Soc.* **1993**, *115*, 7839.

(5) Bowers, M. T., Ed. *Gas-Phase Ion Chemistry*; Academic Press: New York, 1979.

(6) Bouchoux, G.; Houriet, R. *Tetrahedron Lett.* **1984**, *25*, 5755.

(7) Abboud, J. L. M.; Cañada. T.; Homan, H.; Notario, R. Cativiela, C.; Diaz de Villegas, M. D.; Bordejé, M. C.; Mó,O.; Yáñez, M. *J. Am. Chem. Soc.* **1992**, *114*, 4728.

(8) Bordejé, M. C.; Mó,O.; Yáñez, M.; Herreros, M.; Abboud, J. L. M. *J. Am. Chem. Soc.* **1993**, *115*, 73839.

(9) Bouchoux, G.; Drancourt, D.; Leblanc, D.; Mó,O.; Yáñez, M. *New J. Chem.* **1995**, *19*, 1243.

(10) Bouchoux, G.; Leblanc, D.; Mó,O.; Yáñez, M. *J. Org. Chem.* **1997**, *62*, 8439.

(11) Szulejko, J.E.; McMahon, T.B. *Int. J. Mass Spectrom. Ion Processes* **1991**, *109*, 279.

(12) Berthelot, M.; Decouzon, M.; Gal, J.-F.; Laurence, C.; Le Questel, J.-Y.; Maria, P.-C.; Tortajada, J. *J. Org. Chem.* **1991**, *56*, 4490−4494.

(13) Bartmess, J. E.; Georgiadis, R. M. *Vacuum* **1983**, *33*, 149−153.

(14) Miller, K. J.; Savchik, J. *J. Am. Chem. Soc.* **1979**, *101*, 7206−7213. Savchik, J. *J. Am. Chem. Soc.* **1990**, *112*, 8533−8542.

(15) Frisch, M. J.; Trucks, G. W.; Schlegel, H. B.; Gill, P. M. W.; Johnson, B. G.; Robb, M. A.; Cheesemann, J. R.; Keith, T. A.; Petersson,

G. A.; Montgomery, J. A.; Raghavachari, K.; Al-Laham, M. A.; Zakrewski, V. G.; Ortiz, J. V.; Foresman, J. B.; Cioslowski, J.; Stefanov, B. B.; Nanayakkara, A.; Challacombe, M.; Peng, C. Y.; Ayala, P. Y.; Chen, W.; Wong, M. W.; Andres, J. L.; Replogle, E. S.; Gomperts, R.; Martin, R. L.; Fox, D. J.; Binkley, J. S.; Defrees, D. J.; Baker, J.; Stewart, J. P.; Head-Gordon, M.; Gonzales, C.; Pople, J. A. *Gaussian 94 Revision*; Gaussian, Inc.: Pittsburgh, PA, 1995.

(16) Bauschlicher, C. W., Jr. *Chem. Phys. Lett.* **1995**, *246*, 40.

(17) Smith, B. J.; Radom, L. *J. Phys. Chem.* **1995**, *99*, 6468.

(18) Abboud, J. L. M.; Herreros, M.; Notario, R.; Essefar, M.; Mó,O.; Yáñez, M. *J. Am. Chem. Soc*. **1996**, *118*, 1126.

(19) Amekraz, B.; Tortajada, J.; Morizur, J.-P.; González, A. I.; Mó,O.; Yáñez, M.; Leito. I.; Maria, P.-C.; Gal, J.-F *New J. Chem.* **1996**, *20*, 1011.

(20) (a) Bader, R. F. W.; Essen, H. *J. Chem. Phys.* **1984**, *80*, 1943. (b) Bader, R. F. W.; MacDougall, P. J.; Lau, C. D. H. *J. Am. Chem. Soc.* **1984**, *106*, 1594. (c) Bader, R. F. W. *Atoms in Molecules. A Quantum Theory*; Oxford University Press: New York, 1990.

(21) AIMPAC programs package has been provided by J. Cheeseman and R. F. W. Bader.

(22) Farrar, J. M., Saunders, W. H., Jr. Eds. *Techniques for the Study of Ion−Molecule Reactions*; Wiley: New York, 1988.

(23) Benson, S. W. *Thermochemical Kinetics*, 2nd ed.; Wiley: New York, 1976.

(24) Mó,O.; Yáñez, M.; Elguero, J. *J. Chem. Phys.* **1992**, *97*, 6628.

(25) González, L.; Mó,O.; Yáñez, M. *J. Phys. Chem.***,** in press.

(26) Chen, Q.-F.; Stone, J. *J. Phys. Chem.* **1995**, *99*, 1442.

(27) Bouchoux, G.; Choret, N.; Flammang, R. *J. Phys. Chem.* **1997**, *101*, 4271.

(28) Szulejko, J. E.; McMahon, T. B.; Troude, V.; Bouchoux, G.; Audier, H. E. *J. Phys. Chem.***,** in press.